DESIGN, CONSTRUCTION, AND TESTING OF RF STRUCTURES FOR A PROTON LINEAR ACCELERATOR*

E. A. Knapp
University of California, Los Alamos Scientific Laboratory,
Los Alamos, New Mexico

Summary

The factors influencing the choice of a RF accelerating structure for acceleration of protons to high energies in a high-current proton linac are reviewed. Characteristics of resonant periodic cavity chains are described, and the properties of two modes of operation, the π-mode and the $\pi/2$-mode, are discussed. The cloverleaf cavity chain, suitable for use in the π-mode, and four possible configurations suitable for use in the $\pi/2$-mode are described. A new accelerator coupling scheme usable in $\pi/2$-mode tank operation is also discussed. Studies of possible fabrication techniques, and the results of a fabricational program utilizing machined forgings to produce a cloverleaf chain are described. Sparking and electron acceleration tests are also briefly mentioned.

Introduction

Any RF particle accelerator requires an electromagnetic wave traveling with the velocity of the particle and interacting with it to provide the acceleration desired. In a linear accelerator this wave is arranged to travel along a particle's straight line trajectory and to interact almost continuously during the passage of the particle through the machine. Several possible methods exist for generating this traveling wave. In a proton accelerator operating at relatively low energy, the standard approach has been to build a resonant tank loaded with drift tubes which shield the protons from the electric field during field reversal, thereby generating an electric field which has a strong traveling component in the direction of the particle's motion. The technology for designing and building structures of this type is well documented and requires no further discussion. However, as the particle velocity increases, the efficiency of structures of this type for transforming electrical power into particle energy drops rapidly and above proton energies of approximately 200 Mev other methods of generating the interacting wave must be found.

A conventional electron linear accelerator provides a traveling electromagnetic wave at high velocity ($v \approx c$) very efficiently by utilizing a cylindrical waveguide loaded with irises to slow the phase velocity of the traveling wave down to the desired value. In principle, this method could be used to provide the slow waves necessary to accelerate protons from 200 Mev to higher energies. However, in practice slowing the wave to $v \approx 1/3\ c$ requires very heavy loading, so that the structure is not efficient, and control problems become acute with a traveling wave structure in the presence of beam loading.

*Work performed under the auspices of the U. S. Atomic Energy Commission.

Another possibility is to operate the loaded waveguide in a standing wave rather than traveling wave mode. This alleviates the control problems present in the traveling wave mode of operation, but decreases the efficiency of the structure even further. However, operation of a periodic or multiply periodic structure in a resonant mode changes many of the design criteria, and by suitable design the efficiency of a structure of this type may be made very attractive. This report discusses the design, fabrication, and testing of periodic structures suitable for use in a high-current proton linear accelerator, excited in a resonant mode.[1-4]

Among the considerations which must be weighed in developing structures suitable for this use are:

1) Controlability of electric field levels and phases, and thus acceleration rate and particle motions;

2) Efficiency in transferring RF power into particle energy;

3) Freedom from electrical breakdown problems within the cavities;

4) Mechanical tolerance requirements to obtain the required performance;

5) Cost for fabricating these cavities in large numbers.

At Los Alamos we have investigated these factors by a model program, theoretical analyses of the behavior of a chain of coupled resonators, a fabricational program to study possible fabrication techniques suitable for the production of many of these cavities, and a testing program which is investigating some of the problems of beam interaction with the cavities and the high-voltage breakdown of the cavities operating under power.

Design of the cavities has been simplified somewhat by a result of the beam dynamics studies done at LASL, which indicates that for reasonable long tanks (20 $\beta\lambda$ in this case) it is not necessary to change the phase velocity of the traveling component of the electromagnetic wave. Instead, a constant velocity is allowable over this distance. This stepped phase velocity linac then has resonant tanks which may change from tank to tank down the linac, but which are truly periodic within each tank.

In a periodic chain of coupled resonators there are N modes which may be excited if the resonant tank is composed of N cells. Two of these modes, those characterized by a π-radian phase change across a cell boundary and a $\pi/2$-phase

change across a cell boundary, look promising for our purpose. These two modes will be discussed separately, with possible geometries suitable for each, and the properties of each mode.

π-Mode Structures

The conventional choise of operating resonant mode for a periodic chain of cavities is the π-mode, where alternate cavities have the electric field directed in opposite directions at any instant in time. Figure 1 illustrates this mode in a periodically loaded waveguide. Energy coupling in this case is through the axial hole between cavities. π-mode structures which have been considered and modeled at LASL include:

a) Iris-loaded waveguide operating in a standing wave mode;[5]

b) A ventilated or slotted iris waveguide;[6]

c) The cloverleaf accelerator structure;[1,2,7]

d) The crossed-bar structure.[1,8]

To choose a suitable candidate for intensive study from among these structures requires an analysis of the factors affecting the electrical operation of a chain of resonators such as these. An equivalent circuit theory has been formulated which correctly predicts:

a) The mode spectrum and eigenfunctions for a chain of resonators such as the above;

b) The sensitivity of the cavity chains to frequency errors in individual cells;

c) The effects of resonance or near resonance in the coupling mechanism between cavities;

d) Power-flow effects in finite cavity chains;

e) The transient response of a cavity chain to RF drive.

Some of the results of this analysis will be given here, but no systematic development of the results will be shown.[2,4]

The equivalent circuits chosen are the simplest imaginable for the chain of resonators in question, and are shown in Fig. 2a and b. In Fig. 2a an equivalent circuit is shown which would describe a chain of coupled cavities where the coupling elements (slots, holes, etc.) are non-resonant in character, or whose resonant frequencies are sufficiently far removed from the operating frequency to not affect the characteristics of the chain. In Fig. 2b circuits with frequency ω_1 alternate with circuits of frequency ω_2, characterizing a chain where the coupling slots or holes have a resonance near the operating frequency. Typically if ω_2 is within 50% of ω_1, the analysis must be done with the circuit of Fig. 2b to yield meaningful results. The equations derived from the equivalent circuits refer to the resonant frequencies, the resonance widths, field amplitudes and phases, and the coupling strength--quantities which may easily be measured in cavity chains at these frequencies. A rather complete description of the circuit equations, the eigenfunctions and eigenvalues for the chain of coupled resonators, an expression for the phase shift other than π required to transmit power down the system, and perturbation expressions describing the sensitivity of field level to individual cell detuning is found in Refs. 2 and 4. One conclusion that may be drawn from these results is that optimum electrical behavior results from maximum energy coupling from cell to cell in the chain, or maximum mode separation near the π-mode. Maximizing this coupling insures minimum phase changes in the cavity chain due to beam loading, and minimum sensitivity of field levels to tuning errors in individual resonant cells in the chain.

The cloverleaf cavity configuration listed above seems to best fulfill the requirements of optimum mode spacing near π-mode and accelerating efficiency, and has been studied most extensively at Los Alamos. Figure 3 shows a cutaway model of a cloverleaf cavity, modified from the original geometry as suggested in Ref. 7 to optimize its efficiency as a resonant accelerator element. Radial magnetic field lines are generated in the TM010 mode of a cylindrical resonator by deforming the walls into a cloverleaf shape, hence the name cloverleaf. Capacitive loading is added near the axis to increase the transit time factor and decrease the overall size of the cavity. Energy is transmitted from cavity to cavity through 8 radial slots cut in the septum wall between the adjacent cavities. The resonant character of the slots and a rotation of lobes in the adjacent cavities of 45° gives an asymmetric forward wave dispersion curve as shown in Fig. 4. The points on this curve are taken from a 21-cell model made of sheet metal brazed together with an electric torch, after the electric field had been flattened to less than 1% variation. This model is shown in Fig. 5. The solid curve in Fig. 4 is a 3-parameter fit to the dispersion relation

$$(\omega^2-\omega_1^2)(\omega^2-\omega_2^2) = \omega^4 K^2 \cos^2\varphi,$$

where ω_1 is the cell-resonant frequency, ω_2 is the slot resonant frequency, and K is a coupling parameter. This expression is derived from the equivalent circuit analysis, using the circuits shown in Fig. 2b. Other predictions of the equivalent circuit analysis such as the sensitivity of field levels to tuning errors, and the phase shift other than π from cell to cell due to finite Q effects have been investigated and shown to be correct. The asymmetry shown in Fig. 3 gives a large mode separation near π-mode, and thus minimizes the tuning and phase shift problems mentioned above. This asymmetry is produced by the proximity of ω_2 to ω_1, e.g., the slots are near resonance. No other π-mode structures we have investigated show properties nearly as good as the ones observed in these cloverleaf models. Measurements

on a variety of models yield the shunt impedance vs energy curve shown in Fig. 6. A more detailed treatment of the cloverleaf is given in Refs. 2 and 4.

Resonant Coupled Structures

Pi-mode operation means by definition operation at a maxima or minima of the dispersion curve, where mode spacing is small and the group velocity is zero. This operating point has maximum sensitivity to frequency errors in the cells of the chain, and may have large phase shifts other than π from cell to cell due to power flow requirements. Operation at the center of the dispersion curve ($\pi/2$-mode) would alleviate many of these problems but would, if the structure were not altered, reduce the shunt impedance by approximately a factor of two. A scheme for avoiding the shunt impedance reduction while still retaining the $\pi/2$-mode operation was proposed[2] by this group at the MURA Linac Converence last summer and has been studied extensively since.

The properties of the resonant $\pi/2$-mode are unique in that in a chain of identical resonators every other cell stores no energy other than that required to transmit power to make up copper and beam losses. Identical in this context means resonant at the same frequency and nothing else. Thus, every other cell may be of a completely different shape, and so long as it resonates at the same frequency as the "full" or accelerating cell the chain will behave in the $\pi/2$ mode properly.

This is illustrated in Fig. 7 which shows a loaded waveguide operating in the $\pi/2$ standing wave mode, a modification of the loaded waveguide to increase the shunt impedance while still retaining $\pi/2$ mode operation, and an even further modification where the coupling cavity has been completely removed from the beam line and placed off to one side. This displacement of the coupling cavity yields maximum shunt impedance for a given cavity geometry.

Several cavity geometries have been investigated which use this principle to gain high shunt impedance with operation in the $\pi/2$ standing wave mode. Figure 8 shows cutaway views of 4 models we have constructed which operate in this mode. The models of Figs. 8a and 8b have the coupling cavity in line with the accelerating cavity. While the geometry of Fig. 8a does exhibit reasonable shunt impedance and electrical properties, two drawbacks present themselves which tend to discourage this particular geometry compared to other possibilities. These drawbacks are: a) the excessive dimensional tolerance requirements on the short cavity to achieve adequate frequency tolerances for reasonable operation; b) the possibility of beam interaction with the short cavity. Figure 8b shows a cavity chain where the cavity mode in the coupling cavity has been altered so that any possible beam interaction has been removed. Models of this geometry have also been constructed. Good shunt impedance values can be obtained with this system, and behavior is as expected with a $\pi/2$-mode system. Very tight dimensional tolerance requirements are required in the gap of the coupling cell to hold the frequency of the coupling cavity correct in this geometry.

Figure 8c shows a cavity chain utilizing iris coupling to a coupling cavity located to one side of the beam line. Some advantages of this design are: a) low dimensional tolerance requirements on the coupling cavity for adequate frequency tolerance; b) simple geometry; c) maximum shunt impedance, for the coupling cavity is completely removed from the beam line. A 47-cell model (24 accelerating cells, 23 coupling cells) has been constructed with this geometry and the electrical properties investigated. Shunt impedance values in excess of 30 MΩ/m at $\beta = 0.68$ have been observed in models of this type, with ~ 3% bandwidths, gap/cell length = 0.5, hole diameter = 1.5", and f = 805 Mc/sec.

Figure 8d shows a cavity chain utilizing loop coupling into a side cavity. The side cavity is a shorted parallel plate transmission line whose length is set to yield the correct resonant frequency. This system has proven highly successful, showing bandwidths greater than 10% with shunt impedance values of ~ 25 MΩ/m at $\beta = 0.68$, $g/\ell = 0.5$, f = 805 Mc/sec, and $d_H = 1.5$". The one obvious drawback to this structure is the complexity of fabrication required.

The electrical behavior of these systems has been investigated experimentally and also by using the equivalent circuit formulation described previously.[1-4] The equivalent circuit shown in Fig. 2a is adequate for an excellent representation of the properties of the system. The mesh equations

$$I_n = \left\{ 1 - \frac{\omega_{on}^2}{\omega^2} + \frac{j\omega_{on}}{\omega Q} \right\} i_n + \frac{k}{2}(i_{n+1}+i_{n-1}) \quad (1)$$

yield eigenfunctions

$$i_n^q(t) \propto \cos\left(\frac{\pi qn}{N}\right) e^{j\omega_q t}$$

with eigenvalues

$$\omega_q^2 = \frac{\omega_o^2}{1 + k \cos\frac{\pi q}{N}}$$

describing the dispersion curve.

Perturbation theory may be applied to the mesh equations, yielding the sensitivity of the fields to perturbations in cavity frequencies, ω_{on}, coupling constant K_n, etc. For the $\pi/2$ mode we find

$$\frac{\delta i_n^{N/2}}{i_n^{N/2}} = -\frac{1}{K} \sum_{r=1}^{N} \tilde{\varepsilon}_r \frac{W(N/2-r)}{\sin\frac{\pi r}{N}} \sin\frac{\pi}{2} n \sin\frac{\pi rn}{N} \quad (2)$$

where $\tilde{\epsilon}_r$ is the Fourier transform of the cell frequency errors $\omega_{on}^{-2} = \omega_o^{-2}(1-\epsilon_n)$. A similar expression exists for coupling constant errors. An interesting feature of Eq. (2) is that it predicts field amplitudes in the accelerating cells to be independent of frequency errors in the cavity chain (n even). Frequency errors may cause a reduction in shunt impedance by causing larger field values in the coupling cells, as shown in Eq. (2) (n odd). The circuit equations (1) have also been solved numerically on a digital computer with errors in coupling cell resonant frequency, accelerating cell resonant frequency, and coupling constant for various ratios of $Q_{coupling\ cavity}$ to $Q_{accelerating\ cavity}$. Table I summarizes these numerical results for a typical case.

Accelerating cell errors mainly affect the tank effective Q by introducing field into the coupling cells; coupling cell errors introduce phase errors into main cell fields, and coupling constant errors induce tank tilt. These tolerances are extremely loose compared to those for π-mode structure operation. Less than 80-kc cell-to-cell frequency variations should be attainable without requiring excessively tight machining tolerances on individual cavities. Beam loading does not induce phase errors in $\pi/2$-mode operation, it only increases coupling cell fields slightly.

The predictions of the equivalent circuit theory as to tolerance requirements, mode spectrum, cell-to-cell field distributions, phase shifts, and so on have been investigated in the models described and have been found to correctly describe the electrical operation of the system. A more detailed account of our studies of $\pi/2$-mode structures is given in Paper BB-14 by Potter, Knapp, Knapp, and Lucas (this conference).

Recently mesh calculations have been made at this Laboratory which allow calculation of the efficiency and Q of an arbitrarily shaped cavity with cylindrical symmetry (see Paper BB-12, H. C. Hoyt, this conference). These calculations may be used to optimize cavity shape for the cavity chains shown in Fig. 8, insofar as the coupling slots or holes do not appreciably alter the field distributions within the cavities. Figure 9 shows a pair of cavity geometries whose shunt impedance and Q have been calculated in this manner. Shaping the outer wall of the cavity adds 10% to the shunt impedance for this case. Using this computational approach we will optimize the shunt impedance of individual cavities in the chain.

Resonant Coupling with Multiple Drive

The possibility of operating at the center of the dispersion curve where the group velocity is maximum also makes possible another innovation which could relax the tolerances on the RF drive system. If the whole of the accelerator tank is connected together as one long resonator, and modes adjacent to the $\pi/2$ mode supressed by locating the drives at the correct points along the length of the tank, then the phase and amplitude in any tank are controlled by many drives, and drive tolerances are reduced. Figure 10 shows a schematic representation of the proposed system. The gaps between accelerator tanks necessary for quadrupole focusing magnets and valves are bridged by resonant coupling cavities. This effectively ties the whole accelerator together as one long cavity chain. By adjusting the couplings in and out of the bridge cavity it is possible to adjust the relative amplitudes of the fields in adjacent tanks. By adjusting the drive power and bridge couplings, any desired field level can be sustained in a tank regardless of the shunt impedance variations down the length of the accelerator.

Numerical calculations have been performed on a system of 45 resonantly coupled 165-cell tanks, 45 drives periodically spaced along the length of the tanks, where the tanks have $Q_{acc.\ cell} = 20{,}000$, $Q_c = 10{,}000$, $k = 0.04$. There are 7469 cells in the system. Errors were programmed in cell frequencies, coupling constant, and drive phase and amplitude. Both these numerical calculations and analytic solutions indicate phase and amplitude tolerances may be reduced approximately a factor of 5. For a 2° phase 2% amplitude requirement, 10° and 10% are adequate for the amplifier phase and voltage drive, or 10° in phase and 20% in amplifier power. These tolerances are very easy to achieve and could simplify the accelerator greatly. Figure 10 shows computer output for $\pm 10^\circ$ maximum phase error, ±10% maximum drive voltage error, and the listed errors in frequencies. Each tank is tuned to the correct frequency separately in the calculation. More detailed treatment of this proposal is found in Paper F-10 (Knapp, Knapp, Lucas, Nagle, Potter) of this conference.

Fabrication of Waveguide Tanks

If the cloverleaf or other complex structure is to be usable as an accelerator structure, its cost must be reasonable. Both the cloverleaf and resonant coupled structures have a decided advantage over many waveguide structures in that they are relatively insensitive to errors in the frequency of individual cells. This fact made it possible to construct the 21-cell cloverleaf model shown in Fig. 5 by forming the walls over simple wooden dies and welding the assembly together. Tolerances of about 0.005" seem adequate for the cloverleaf cavities for all dimensions except the gap between drift tubes, which should be held to ~ 0.001". These dimensions should make final tuning relatively simple.

After investigating a large number of possible fabricational techniques and discussing the materials problems with a number of possible suppliers, a method of production which appeared to be the most economical was decided upon. First, solid OFHC copper construction with silver brazed joints was chosen for reasons of electrical conductivity and vacuum integrity. The approximate cloverleaf shape was produced by making OFHC copper forgings whose dimensions required approximately 0.1 inch of copper to be removed to arrive at the design dimension. These have been produced

very economically by standard forging techniques. A photograph of a forging is shown in Fig. 11. The forging is of two half cells with the septum separating the cells in the center of the forging. The void behind the wall indentation is used as the water-cooling passage in the final cavity. These forgings are then machined to the required tolerances using a series of machining operations which include lathe work around the drift tube and tracer-mill work on the outside wall. The finished machined part is shown in Fig. 12. These parts are then assembled with a silver-brazing alloy in the joint at the center of each cell and brazed in a hydrogen atmosphere. So far a one plus 2-half cell model has been made in this way and it is very satisfactory. Production of a 40-cell accelerator tank mock-up is underway and should be completed by April 1965. This tank will be tuned by deforming the noses inside the water passages to change the frequency of individual cells, while field levels will be measured using standard perturbation techniques. Fabrication of the resonantly coupled structure using these techniques should be simpler than the cloverleaf.

Accelerator Structure Testing

Sparking Tests

The one plus 2-half cell model constructed using the machined forgings described above has been used to investigate RF field breakdown problems in the cloverleaf cavity. With the measured shunt impedance of this cavity 25 kw of peak RF power drives the cavity to design voltage level (~ 1.2 Mv/m particle energy gain). This cavity has been driven up to 100-kw peak power with no sustained sparking observed. Some x-ray emission was noted but appears to be associated to some degree with surface contamination. (See Paper BB-13, Parker, Doss, Freyman, Knapp, Shlaer - this conference.)

Beam Acceleration Tests

A chopped electron beam has been passed through the 21-cell cloverleaf tank shown in Fig. 5 and the peak electron energy gain measured as a function of RF drive power. This experiment will be described fully in a later paper. (See B-9, Brolley, Emigh, Mueller - this conference.) However, results indicate no adverse modes are excited by a beam pulse with shape and spacing very similar to that anticipated in the linear accelerator. These measurements were taken at approximately the analog beam current of the proton case. The extension of these measurements to investigate beam blow-up phenomena, space-charge effects and so on is underway.

Acknowledgments

The work reported here is certainly the result of a joint effort of many people. I would like to thank D. E. Nagle especially for his constant advice and help during the course of these measurements. B. C. Knapp was indispensable during the course of the work on both $\pi/2$- and π-mode structures, and was responsible for many of the ideas mentioned. The success of the cloverleaf fabrication program is primarily due to the efforts of H. G. Worstell. R. R. Sharp, R. J. Bueschel, and W. H. Yeamans have done an excellent job of fabricating the models used in our testing program. G. J. Lucas and J. M. Potter have contributed greatly to the equivalent circuit analysis and studies of $\pi/2$-mode structures. D. C. Hagerman, J. R. Parker, J. D. Doss, and R. W. Freyman have constructed the 100-kw power amplifier and done most of the sparking tests. J. E. Brolley, C. R. Emigh, D. W. Mueller, and D. D. Armstrong are responsible for the electron model experiments.

References

1. E. A. Knapp, Proceedings of the Yale Conference on Proton Linear Accelerators, 1963.
2. E. A. Knapp, Proceedings of the MURA Conference on Linear Accelerators, 1964.
3. D. E. Nagle and E. A. Knapp, Proceedings of the Yale Conference on Proton Linear Accelerators, 1963.
4. D. E. Nagle, Proceedings of the MURA Conference on Linear Accelerators, 1964.
5. M. Chodorow et al., Rev. Sci. Instr., Vol. 26, 134 (1955).
6. S. Giordano, Proceedings of the Yale Conference on Proton Linear Accelerators, 1963.
7. M. Chodorow and R. D. Craig, Proc. IRE, Vol. 45, 1106 (1957).
8. A. Carne, Proceedings of the Yale Conference on Proton Linear Accelerators, 1963.

TABLE I

FREQUENCY AND COUPLING CONSTANT TOLERANCES, $\pi/2$ MODE

f = 805 Mc/sec
Q_{ac} = 20,000
Q_{cc} = 10,000
k = 0.04

161-cell tank
81 accelerating cells
80 coupling cells

Square error distribution, with half-width δ.

$\delta f_{acc.\ cell}$	$\delta f_{coupling\ cell}$	$\frac{\delta K}{K}$	Q_{eff}	Max. Tank Tilt	Max. Phase Diff.
0	0	0	19,931	1%	0°
80 kc	80 kc	0.1%	19,924	1.5%	0.46°
240 kc	240 kc	0.1%	19,902	1.6%	0.78°
800 kc	800 kc	1.0%	19,185	10 %	2.21°

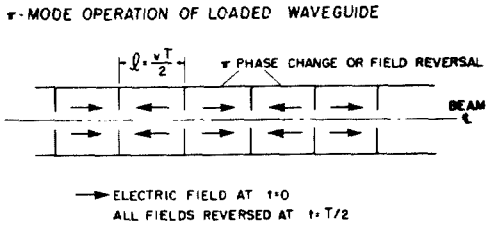

Fig. 1. π-mode operation of a periodic chain of cavities.

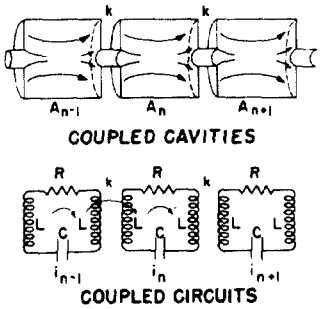

a. Equivalent circuit for a non-resonantly coupled periodic chain of resonators.

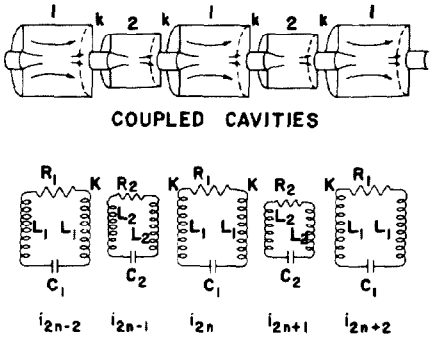

b. Equivalent circuit for a multiply periodic chain of resonant cavities, with alternating frequencies ω_1 and ω_2. Cells with ω_1 may characterize the accelerating cavities, cells with ω_2 the coupling cavities or slots.

Fig. 2.

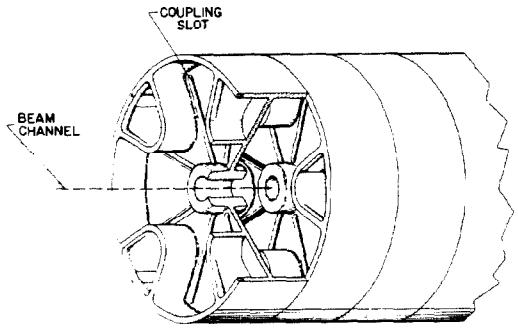

Fig. 3. Cutaway drawing of a cloverleaf cavity chain.

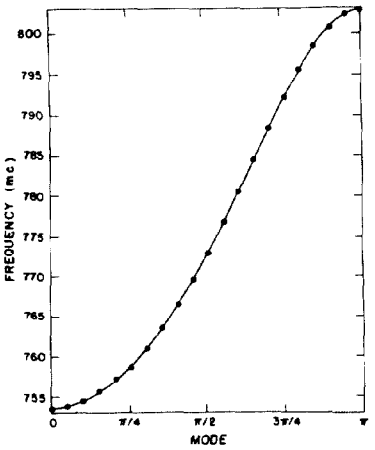

Fig. 4. Measured dispersion curve for a 21-cell cloverleaf accelerator tank. The solid line is a least squares fit to the three parameter dispersion relation derived from the equivalent circuit theory for a multiply periodic cavity chain.

Fig. 5. 21-cell cloverleaf model built of sheet copper formed over dies and heliarc brazed.

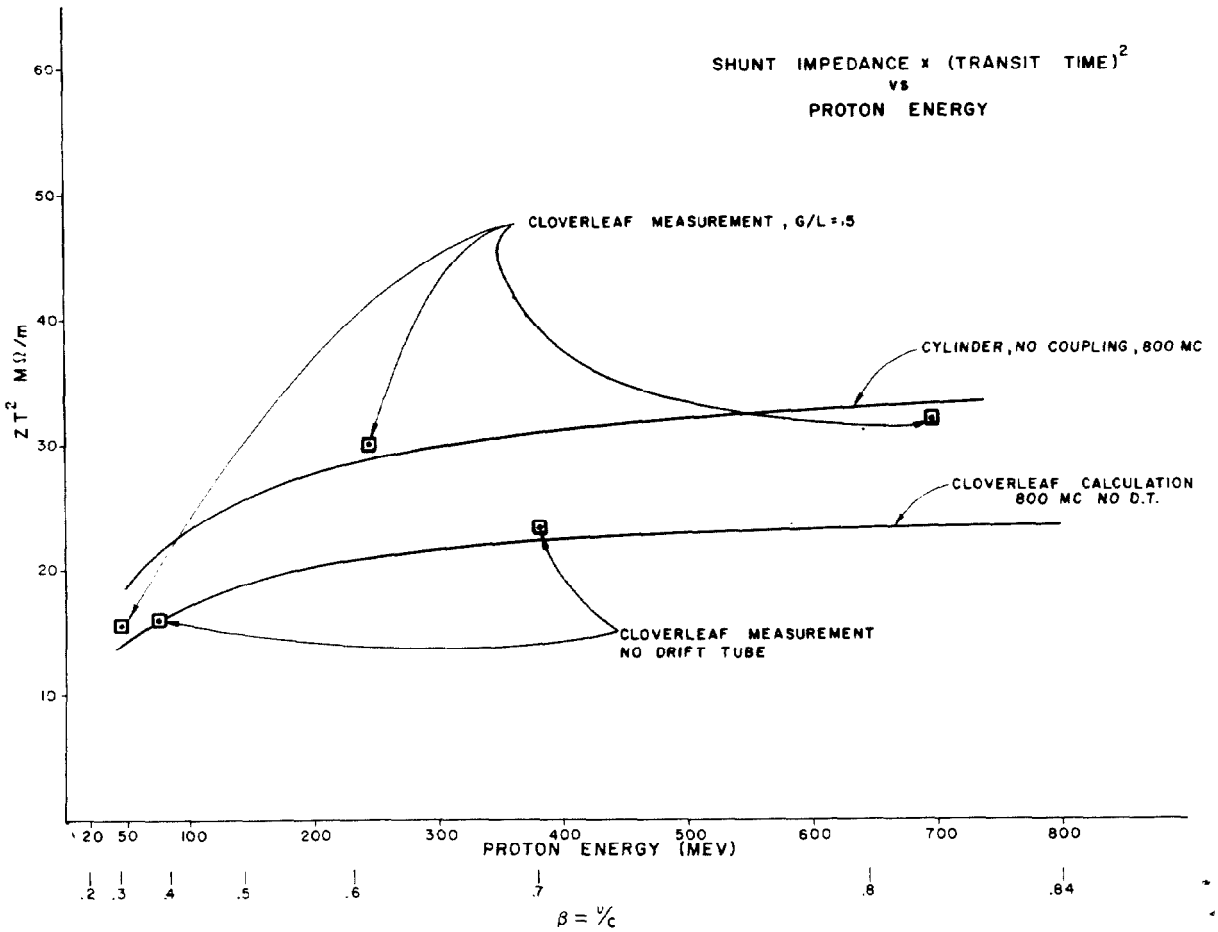

Fig. 6. Shunt impedance vs energy for the cloverleaf cavity chain.

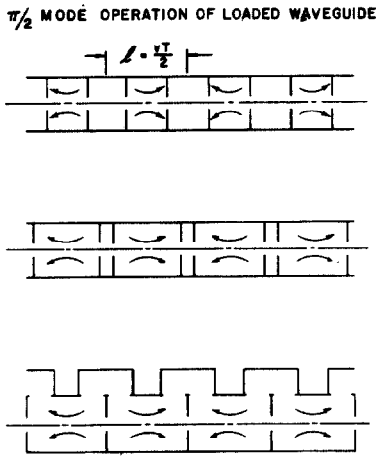

Fig. 7. $\pi/2$-mode operation of a loaded waveguide, a modification of a loaded waveguide to provide increased shunt impedance, and a further modification removing the coupling cavity from the beam line while retaining $\pi/2$-mode operation.

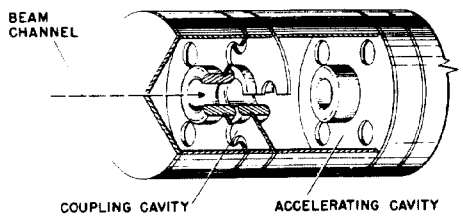

Figure 8a.

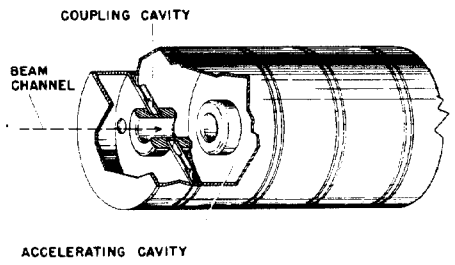

Figure 8b.

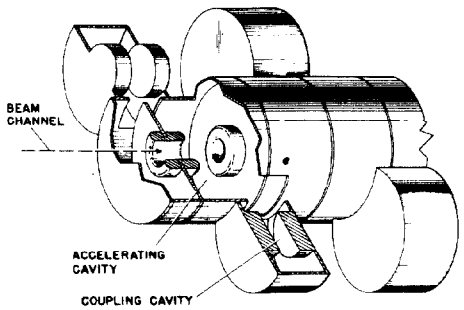

Figure 8c.

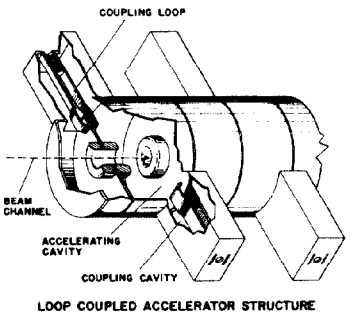

Figure 8d.

Fig. 8. a-d. Four models constructed which operate in $\pi/2$-resonant mode.

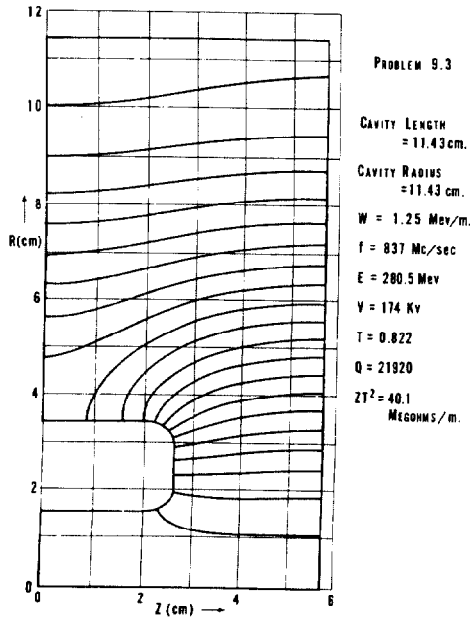

Figure 9a.

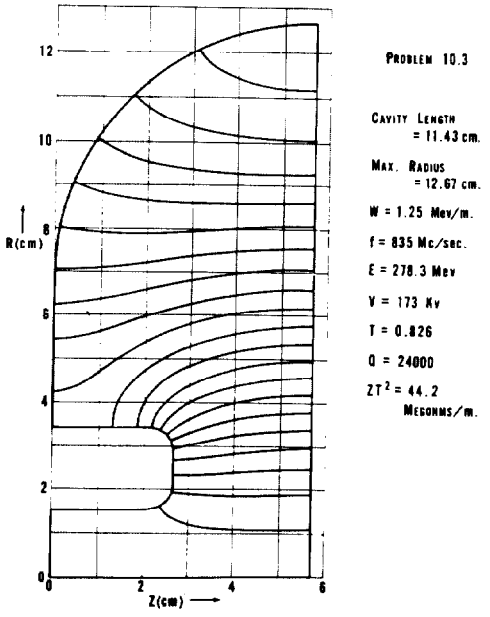

Figure 9b.

Fig. 9. Mesh calculation of the shunt impedance and Q for a cavity with cylindrical symmetry. A cross section of the upper left quadrant is shown. The lines define surfaces of constant F = rH.

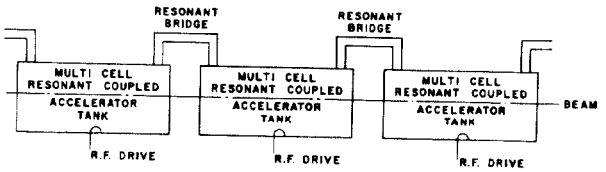

Fig. 10. System for a multiple drive of a resonantly coupled multitank accelerator with tank-to-tank coupling.

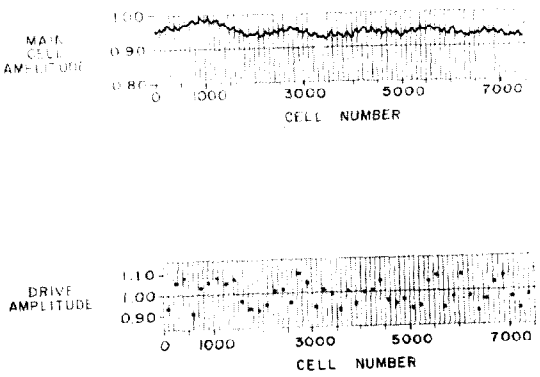

Fig. 11. Cell amplitude and phase for a 7469 cell resonant coupled accelerator tank driven at 45 points. Cell frequency errors are random within a square distribution 160 kc wide, coupling constant errors are random within ± 0.1%, and drive amplitude and phase errors are random within ± 10% and ± 10°.

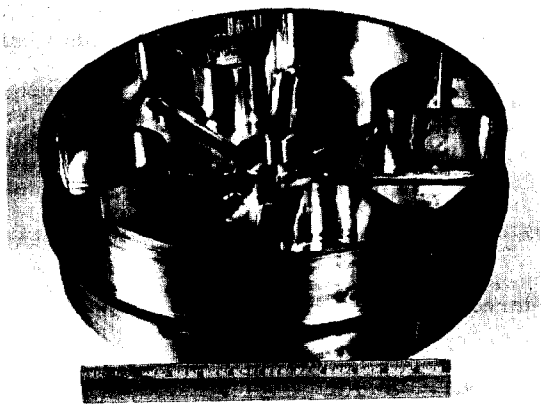

Fig. 13. Finished cloverleaf cavity unit.

Fig. 12. OFHC copper forging in the cloverleaf shape.